Identifying Novel Aging-Related Biomarkers for Age-related Macular Degeneration with Integrative Bioinformatics Approaches

Liangchuer Zhao[1,a,*]

[1]*Chongqing DEPU Foreign Language School, Chongqing, China*
a. zhaoliangchuer@163offer.com
*corresponding author

Abstract: Age-related macular degeneration (AMD) is the leading cause of visual impairment in older adults worldwide and is a condition that causes visual deprivation. There exist two subcategories of this disease with the wet form of this disease being the focus of our study. Using bioinformatic analysis, this research conducted investigations to uncover the genes related to aging that may be biomarkers for the development of AMD. First, we compared the expression levels of samples from AMD/CNV patients and a control group using the GEO microarrays (GSE29801) in order to obtain differentially expressed genes (DEGs). WGCNA, combined with functional enrichment analysis, is utilized to discover and validate the gene module crucial for AMD. Differentially expressed aging-related genes (DEARGs) were identified by overlapping significant gene sets. The subcellular location of hub DEARGs and their corresponding cell subpopulations were determined and predicted using the Geo dataset GSE155288. Pan-cancer analyses were used to confirm those hub DEARGs' function in other diseases. Moreover, both Protein-Protein Interaction (PPI) and AlphaFold prediction were employed to validate the protein interaction among the key DEARGs. Lastly, a potential target drug was selected, with portions of them validated through drug-protein interactions. In further analysis of our result, the collect gene set of 7 DEARGs was divided into the immune-related group and the non-immune-related group. These groups uncovered two distinct pathways of AMD development, with one triggering inflammatory responses by promoting macrophage proliferation and the other inducing choroidal neovascularization formation due to malfunctioning growth regulator genes.

Keywords: Age-related macular degeneration (AMD), Age-related gene, transcriptomics

1. Introduction

Age-related macular degeneration (AMD), often simply referred to as AMD, is a degenerative disease that is a primary cause of blindness among the elderly and the leading cause of visual impairment worldwide. It significantly contributes to the decline in vision among aging populations globally and severely impacts their quality of life [1]. Studies indicate that AMD is responsible for approximately 6% to 9% of cases of legal blindness globally, with a third of all vision loss attributed to this condition [2-4]. AMD is characterized by pathological cell death within the inner retinal layers of the macula and the surrounding blood vessels, leading to a loss of central vision. The affected layers include the

photoreceptor layer, the retinal pigment epithelium (RPE), the collagen-rich Bruch's membrane, and the choriocapillaris, which is the innermost layer of the capillary network [5]. The disease presents in two distinct forms: the 'dry' form and the 'wet' or neovascular form. Dry AMD is the more common form, representing 85-90% of all cases, and it has the potential to progress to wet AMD, which accounts for 10-15% of all cases [6]. Wet AMD is characterized by hemorrhaging and exudation in the macular area of the retina, caused by the growth of choroidal neovascular membranes (CNV) [7, 8]. This can lead to retinal bleeding, detachment or atrophy of the RPE, accumulation of hard exudates, and sub-retinal fluid, all of which can result in permanent vision loss [9]. Inflammation is increasingly recognized as a significant contributor to the etiology of wet AMD [10], compromising visual clarity. The neovascular form of AMD will be the focus of further discussion in this research.

Among the causes of AMD, aging is the dominating pathogenesis [11, 12]. Aging is a gradual and irreversible pathological process. The effects of aging include mitochondrial dysfunction and loss of proteostasis [13], and for the eyes, increased blood vessel resistance, decreased choriocapillaris density, lipid and lipoprotein accumulation in the Bruch membrane, and decreased photoreceptor density are all consequences of aging [14]. Immune system dysregulation, also associated with age, is known as immunological aging and is characterized by compromised immune responses and excessive inflammation [15]. Thus, it is revealed that the AMD patients' complement system has consequently minor capability of modulating inflammatory responses, which would result in superfluous cell damage with extracellular waste accumulation [16], underlying the expression differences in AMD disease. The significance of identifying an age-related macular degeneration (AMD) biomarker is underscored by its assistance in revealing the causes of diseases and its offers of potential ideas for therapeutic interventions. Specifically, wet AMD is a heterogeneous disease, and although its manifestation is clinically the same in different patients[1], the molecular mechanisms behind it are different, which will also lead to patients having different responses to the same treatment techniques. Meanwhile, despite the obvious manifestation of aging as an approved pathogenesis of AMD, the underlying molecular mechanism remains a question yet to be solved. Hence, bringing forth an aging-related biomarker identification of AMD can make potential construction of the cause of aging on AMD. From another therapeutic point of view, at present, the most commonly used and most effective treatment for wet AMD is the injection of an anti-angiogenesis drug, such as the anti-VEGF therapy[2]. However, this treatment direction does not address the cause of AMD due to aging, and long-term injection is needed to maintain a healthy status[3]. Thus, identifying that aging-related AMD marker could also direct a potential future therapeutic direction for the disease.

The study of AMD through experimental methods remains a specialized field, with the procurement of human retina specimens being a significant challenge that limits the number of studies with experimental data. Among the few datasets in the research of AMD, two were selected for our research due to our lack of access to AMD patient samples. Hence, we conducted a series of bioinformatic analyses to identify unique gene expression patterns associated with AMD and conducted validation testing to find genes linked to aging that may serve as biomarkers for the pathogenesis of AMD.

2.   Methods

The goal of this research is to find potential biomarkers for age-related macular degeneration (AMD) by concentrating on age-related genes that are essential to the onset of the condition, as shown in Figure 1. The comprehensive process of this research is outlined in the accompanying diagram, which illustrates the systematic approach taken to analyze and validate the genes associated with aging that may serve as biomarkers for AMD.
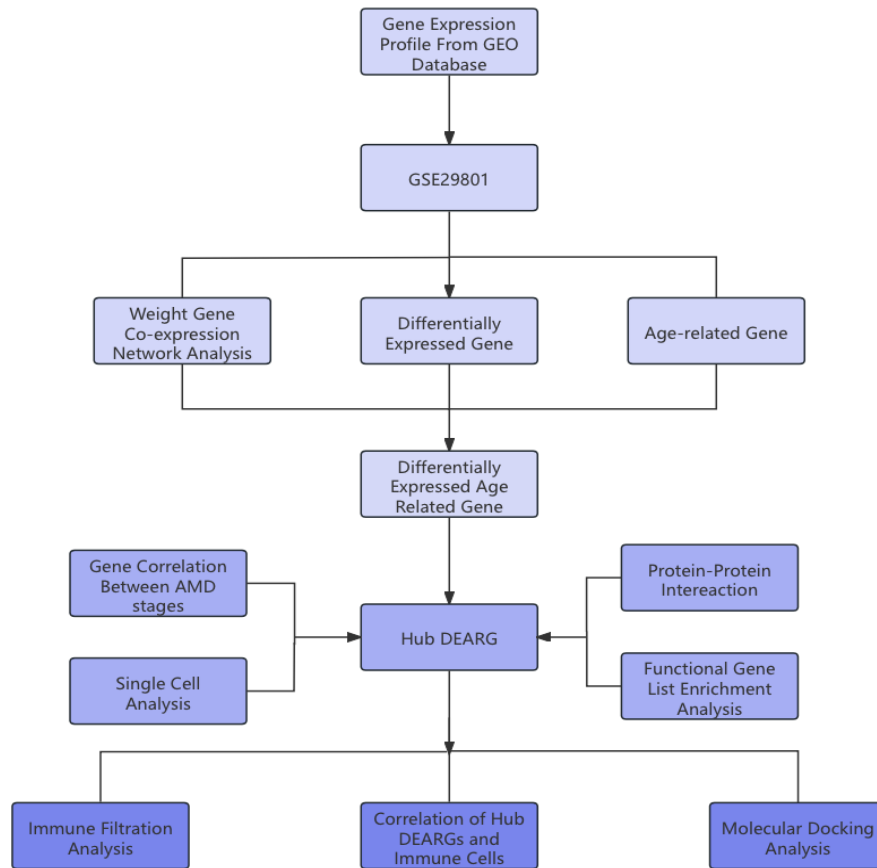
Figure 1: Flowchart of the AMD Study Utilizing Integrative Bioinformatics Approaches.

2.1. Identification of Aging-Related Genes (ARGs) and Differentially Expressed Genes (DEGs) in AMD

To obtain data for identifying the differentially expressed genes in AMD, this research chooses to search for publicly available data instead of conducting a first-hand experiment due to the difficulty of accessing samples. Thus forward, from the openly accessible GEO database[4], we were able to get the expression profiles of AMD patients' genes. For the transcriptome analysis at the systems level of the retina and retinal pigmented epithelium (RPE)-choroid complex, dataset GSE29801 was chosen. The used samples were gathered from the University of Iowa (GSH) and the Lions Eye Bank of Oregon, and the results were generated from 26 AMD, 31 normal, and 11 latent pre-AMD human eyes. In need of specificizing the data, this research chose to use the samples derived from wet AMD (CNV) patients and normal people, in a total of 9 CNV samples and 50 normal sample tissues. Following the extraction, the log2 transformation was used to standardize the extracted data. The normalized quantiles function of the preprocessor package in the R software (version 3.4.1) was utilized to normalize the microarray data. Using $|Fold\ Change\ (FC)| > 1$ a $corrected\ p - value < 0.05$ as the screening threshold, the differentially expressed gene (DEGs) is identified. The five most differentially expressed genes were annotated according to their information on GeneCards – the human gene database (www.genecards.org). Furthermore, to reinsure the relationship with aging, we extracted 1357 genes with a relevance score of more than five from the GeneCards database to obtain age-related genes (ARGs). These ARGs were preserved for the following analysis.

2.2. Application of Weighted Gene Co-expression Network Analysis (WGCNA) for Identifying Clinically Significant Modules

Subsequently, we employed Weighted Gene Co-expression Network Analysis (WGCNA) to further identify significant gene clusters. The intention of this method is to identify gene modules that are highly linked and could be important in the onset of age-related macular degeneration (AMD). The raw data for this section consisted of the results from the expression differentiation analysis, with outliers having been identified and excluded. Utilizing the R package "WGCNA" [5], we pinpointed modules that are most significantly associated with AMD. This analytical method is initiated by constructing a genetic correlation network, which quantifies the concordance of gene expression levels using Pearson correlation coefficients. Then, through dynamic tree cutting, clusters exhibiting similar expression patterns are segregated and consolidated into distinct modules [6]. Subsequent gene enrichment analysis and gene significance comparisons can then elucidate the most impactful gene cluster related to the disease, aiding in the identification of the key module. For the analysis, outlier samples were removed. After cluster identification, we selected the prominent cluster from the gene network based on a p-value threshold of less than 0.05. The selected modules were retained for further in-depth analysis.

2.3. Identification and Annotation of DEARGs through Functional Gene Enrichment Analysis

Since there was no predetermined module, functional enrichment analysis was used to determine which module is essential to AMD progression. We employed the overrepresentation analysis (ORA) approach, utilizing Fisher's exact test and the Hypergeometric distribution test, followed by consultations with the DAVID database, specifically DAVID Bioinformatics Resources version 6.8. Subsequently, we utilized the Kyoto Encyclopedia of Genes and Genomes (KEGG) pathways, the PANTHER database, and Gene Ontology (GO) enrichment analyses to determine the associated pathways of the modules, including explorations into the KEGG disease database. The enrichment results allowed us to pinpoint and retain the most relevant module. We then utilized the online platform at https://www.bioinformatics.com.cn (last accessed on October 10, 2024) to generate an enrichment scatter plot. Through this analysis, we identified and preserved the most relevant module. Subsequently, we constructed a Venn diagram to intersect significant modules, identify ARGs and DEGs, and compile a list of DEGs that were significantly associated with both AMD and aging. These genes were termed differentially expressed age-related genes (DEARGs). Further enrichment analyses were conducted on the DEARGs to elucidate the functions of this gene cluster. We defined significant enrichment as having a corrected p-value less than 0.05, and any results outside this threshold were discarded. Finally, we investigated the functional annotations of each gene within the DEARGs using the GeneCards database and presented their information in the following table.

2.4. Single-Cell Analysis and Identification of Subcellular Localization for Hub DEARGs

Next, the precise location of the hub DEARGs was searched using single-cell transcriptome profiling. The raw data used orients from the dataset GSE155288 in the Gene Expression Omnibus (GEO) database (https://www.ncbi.nlm.nih.gov/geo/) and following the elimination of low-quality cells using the Seurat package, we performed the standard data preprocessing steps. The standard analysis was conducted using the corrected-normalized data metrics, following instructions provided in the Seurat R package. For the principal component analysis (PCA), 10 top variable genes were extracted. tSNE_1 was used, where the algorithm reduces the raw RNA-seq data which is high dimensional, to a low two-dimensional graph. We utilized the function FindClusters included in the Seurat R package as the cell clustering was carried out[9] The top 10 components were retained to be revealed on the

cluster graph. Furthermore, the expression level of the different hub genes was also explored between the identified clusters. Hence, the biomarker gene subcellular localizations were predicted. Using the COMPARTMENT database (https://compartments.jensenlab.org/), we explored the precise subcellular location for the protein of each of the genes. This website offers localization analysis of proteins from data obtained in multiple protein databases and past literature.

2.5. Comparative Analysis of Immune Cell Infiltration in Control Subjects and AMD Patients

Owing to the importance of inflammation during the process of AMD, we decided to study the expression of immune cells in the DEARGs of this disease. We received the immune cell infiltration abundance raw data from 24 gene expression datasets and used the RNA-Seq and microarray data. Analysis was based on a single sample Gene Set Enrichment Analysis (ssGSEA) algorithm, contained inside the R package of ImmuneCellAI[10]. By determining the ssGSEA enrichment score of the expression deviation profile of the hub DEARGs, the abundance of them in immune cells was projected. An enrichment ratio diagram was generated to illustrate the proportion of each immune cell type across the individual samples, and a box plot was drawn to reveal the correlation of the 24 different immune cell types with the hub genes.

2.6. Correlation and Pan-Cancer Analysis of Immune-Related Hub Genes and Infiltrating Immune Cells

Additionally, we looked into the relationship between immune cells and each hub gene. First, the clinical data that corresponded to the RNA-sequencing expression (level 3) profiles for Pan cancer, originating from the TCGA dataset (https://portal.gdc.com). We employed immuneeconv to evaluate the immune score evaluation's dependable outcomes. CIBERSORT[11] is one of the six most recent algorithms integrated into this R software package and was used in this analysis. In the presentation of results, R 4.0.3 was used to implement the R package and all of the analysis techniques. Next, we used the GEPIA2 analytic tool [12] to show the expression difference between the two hub genes, which are related to immunity, in a variety of cancer types. The results show the level of expression difference in a scatter diagram, where up-regulation is marked red and down-regulation is marked green.

2.7. Identification of Significant Networks through Protein-Protein Interaction (PPI) Analysis and Protein Domain Visualization

Next, we used PPI analysis to find the Hub DEARG interaction network. How the hub DEARGs interacted with each other was investigated through The STRING database, with the results filtered through the criteria intereaction score > 0.4 and $p-\text{value} < 0.05$ Afterward, we went in search of the details protein domains that those interactions may potentially be exhibiting in. To do so, we collected data from protein databases Uniprot[13] and Ensembl[14], then used the online tool SMART to reveal the domain in the interacting proteins. We then used Domain Graph, version 1.0 (DOG) to visualize the proteins with domains annotated.

2.8. Protein-Protein Interaction Prediction Utilizing AlphaFold

To study the details of the hub gene network interaction, we used AlphaFold server[15] to create a model of the protein and predict their combining structure and interactions. After retrieving the protein sequence from Uniprot, the corresponding structure was computed and the configuration was

then modified using The PyMOL Molecular Graphics System, Version 3.0 Schrödinger, LLC where the interacting bonds and residue locations were highlighted.

2.9. Drug-Protein Interaction Analysis via Molecular Docking and Target Drug Selection for DEARGs

PubChem database[16] (https://pubchem.ncbi.nlm.nih.gov/) and PharmaProjects (https://citeline. informa.com/) were utilized in the finding of potential therapeutic drugs for targeting the identified hub genes. The drug-protein interaction was then investigated with the protein structures and drugs that have\ activity\ type=IC50(EC50) and activity\ value<0.05\mu M. Using silico protein-ligand docking software AutodockVina 1.2.2[17], the binding affinities and mechanisms of interaction were examined. The PDBQT formatted protein and molecular data were transformed before docking analysis by adding polar hydrogen atoms and removing all water molecules. The grid point distance was 0.05 nm, while the grid box dimensions were set at 30 Å × 30 Å × 30 Å. The molecular docking was carried out using Autodock Vina 1.2.2 (http://autodock.scripps.edu/).

3. Results

3.1. Identification and Functional Enrichment Analysis of DEGs in AMD

Genes that exhibit differential expression between normal individuals and AMD patients were identified by processing of the data obtained from GSE29801; these genes will be referred to as DEGs. According to the filtering standard $|\text{Fold change} (FC)| > 1$ and $p - \text{value} < 0.05$, 103 genes were shown to be significantly associated with AMD. (Figure 2A). A heatmap was draw to show the difference between the difference in expression between the CNV/AMD patients and the control (Figure 2B). Among these, only 7 genes were up-regulated while the other 96 genes were down-regulated. The top five most differentially expressed genes were enlisted in the chart below, along with their respective annotations from GeneCard (Table 1). Next, functional enrichment analysis was performed which included the use of the KEGG pathway, GO term, and PANTHER database. The results show these DEGs were associated with various pathways, the most prominent being angiogenesis, apoptosis signaling pathway, inflammation mediated by chemokine along with cytokine signaling pathway, vitamin D metabolism, and pathway. A large enrichment value from the PANTHER database demonstrated that inflammatory and immune responses are strongly correlated with these DEGs, along with the apoptosis signaling pathway, the chemokine and cytokine signaling pathways, and more interestingly, angiogenesis signaling pathways were significantly enriched in this study (Figure 2C). These processes were highly related to the disease AMD and could also ensure the dependability of our data.

However, the results gathered from the GO database show a different perspective of the DEGs for the top 10 analyses were mainly associated with growth, including multicellular organism development, system development, response to growth factors, and animal organ development (Figure 2D). In addition, further results from GO term show that pathways related to the eye and the nervous system were also enriched, which were visual perception and sensory perception of light stimulus (Figure 2D). As for the enrichment of the KEGG pathway, results are categorized into 4 sections according to similarities in pathways. Specifically, it shows that these DEGs may be related to immune response pathways, viral protein interaction with cytosine and cytosine receptors, ECM-receptor interaction, and IL-17 signaling pathway were all enriched (Figure 2E). The findings above evidently support the idea that the inflammation process and growth development are key components of AMD development, with immunology as a relatively minor portion.
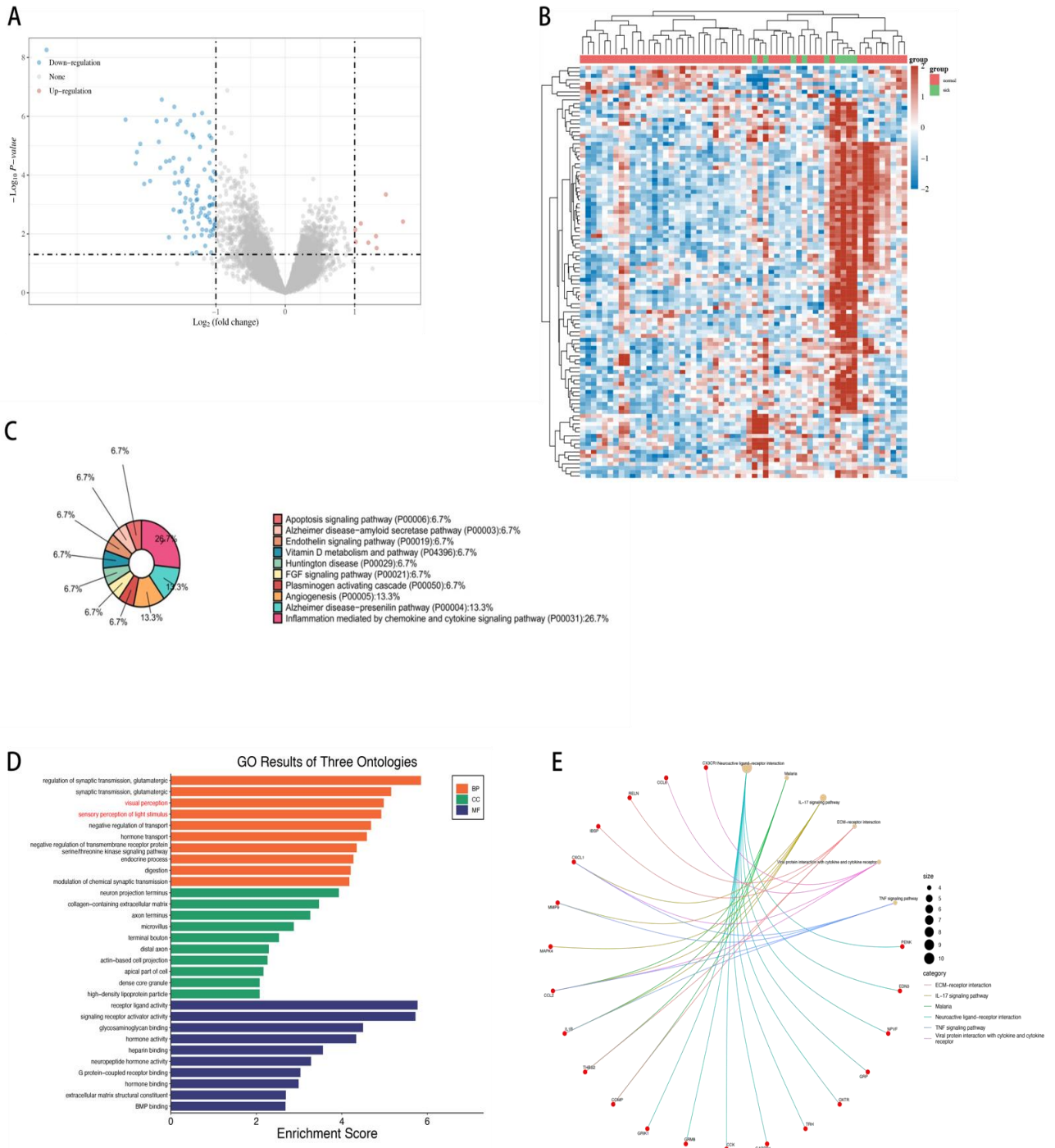
Figure 2: Identification and Functional Enrichment Analysis of DEGs in AMD.(A) Volcano plots and (B) a cluster heatmap depicting the DEGs resulting from the comparison between AMD patients and controls. (C) Enrichment results obtained from the PANTHER database, (D) Gene Ontology (GO) databases, and (E) Kyoto Encyclopedia of Genes and Genomes (KEGG) database for the DEGs.

Table 1: Top Five DEGs in AMD and Their Annotations

Gene Symbol	logFC	Function
NPVF	-3.439549034	Strong negative regulator of gonadotropin synthesis and secretion
S100A2	-2.301191088	Supports cellular calcium signaling by acting as a calcium sensor and modulator.
CHST2	-2.155387224	Functions as SELL ligands and is essential for lymphocyte homing at inflammatory areas.
NCAN	-2.137195618	Bind to neural cell adhesion molecules to regulate neurite formation and neuronal adhesion throughout development.
FDCSP	-2.089270031	Bind to B-lymphoma cell surfaces and act as a secreted mediator.

3.2. Application of Weighted Gene Co-Expression Network Analysis to Identify Significant Modules

For the search for biomarkers of AMD, identifying the gene modules most closely related to the disease AMD in the gene correlation network could further narrow the profiling criteria. Hence, WGCNA is used with the eigengene data from the prior gene expression data. A soft threshold standing at a value of 7, where R^2 equals 0.85, was used to fabricate a scale-free network. (Figure 3A). A sample dendrogram was then drawn and the outlier samples were discarded from further procedures (Figure 3B). Then, on the basis of dynamic tree clipping and average hierarchical clustering, 11 modules were detected, where each module is represented with a specific color with the exception of grey (Figure 3C). Following the clustering of module feature vectors, an analysis of clusters where the distance between them is consistent with their relativity (Figure 3D). After this, the correlation of the modules with clinical features was explored, where in this case, group 1 consists of normal people while group 2 consists of AMD patients (Figure 3E). The modules with the strongest correlation to AMD were identified, taking the modules blue and green as the most significant modules with blue as the more prominent one (Figure 3F, G).

In order to select the more crucial gene module, the comparison of each module's functional enrichment analysis is carried out. Through KEGG analysis, it is found that blue is associated with eye disease and congenital malformation of the eye, which is highly consistent with the target disease of this research (Figure 3H). Meanwhile, the green module showed less intriguing and irrelevant results, where its enrichment pathways were of little relation to the disease AMD (Figure 3I). Hence, the blue module is selected as the most significant module, and further enrichment results of blue confirmed our choice of it. In a more detailed GO analysis result (Figure 3J), the blue module was enriched for presynaptic calcium ion concentration regulation, retinal layer formation, and neural retinal development. More significantly, the biological pathways associated with development such as neuron development, visual system development, eye development, and multicellular organismal process were also included in the function of the blue module.
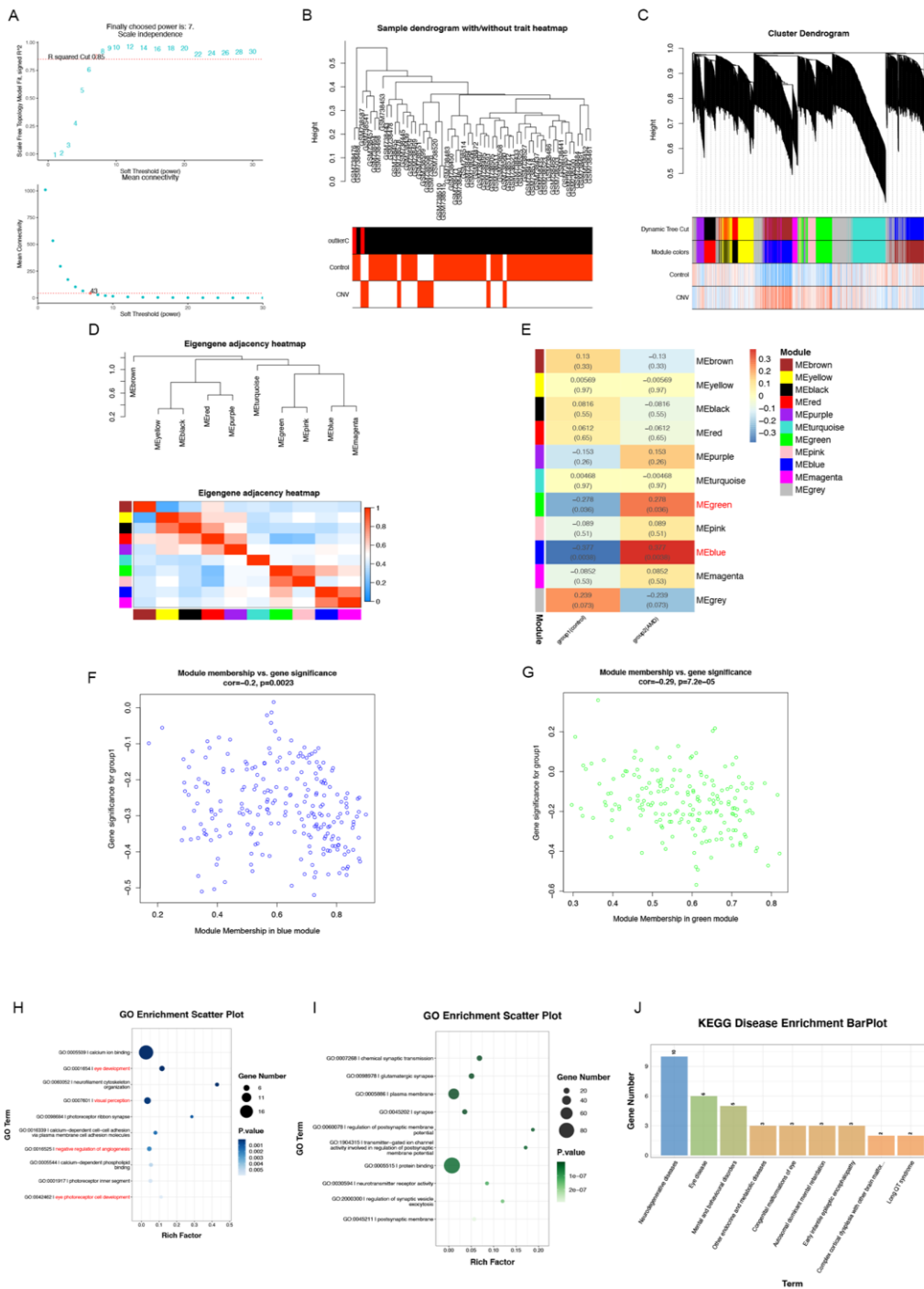
Figure 3: Developing a Weighted Gene Co-expression Network and Finding Clinically Important AMD Modules. (A) Determination of the soft threshold value for subsequent analysis. (B) Clustering dendrogram with each sample's tree leaf corresponding to the identification and elimination of outlier samples. (C) Cluster dendrogram displays each cluster in a unique color. (D) Heatmap illustrating the correlation and connection between each cluster module. (E) Heatmap depicting the association between AMD clinical characteristics and module eigengenes. (F) Correlation between AMD gene importance and blue module membership visualized using a correlation scatter plot. (G) Correlation between AMD gene importance and green module membership visualized using a correlation scatter plot. (H) KEGG enrichment analysis of the blue module. (I) KEGG enrichment analysis of the green module. (J) Further Gene Ontology (GO) enrichment analysis of the blue module.

3.3. Identification and Functional Annotation of DEARGs in AMD

By intersecting the differentially expressed genes (DEGs) and aging-related genes from the WGCNA blue module, we constructed a Venn diagram that revealed a common set of 7 genes (Figure 4A). To validate the significance of this group of DEARGs (Differential Expressed Aging-Related Genes), we conducted an enrichment analysis using the KEGG disease database (Figure 4B). The results demonstrated a substantial link between these genes and eye disease pathways, with AMD, congenital eye malformations, and cataracts being the most enriched pathways, all of which are closely related to AMD. This confirms the relevance of this group of DEARGs in the context of AMD. Furthermore, PANTHER pathway analysis (Figure 4C) uncovered additional related pathways, such as angiogenesis, the plasminogen activation cascade, inflammation mediated by chemokine and cytokine pathways, and the apoptosis signaling pathway. Notably, Vitamin D metabolism and the FGF signaling pathway were also enriched, emphasizing the significance of genes associated with growth and development within this overlapping gene set. An analysis of the correlation between these hub genes revealed a predominance of positive correlations, with only a few negative ones (Figure 4D). Consequently, the DEARGs were identified, and their identity and functional annotation are presented in the table below. The annotation results substantiate their association with AMD (Table 2).

Table 2: Identification and Functional Annotation of DEARGs

Gene Symbol	Functional Annotation
APOC1	inhibitor of lipoprotein binding to the receptors for very low-density lipoprotein (VLDL), low density lipoprotein (LDL), and LDL receptor-related protein.
CALB1	Vitamin D-dependent Calcium binding protein
CRB1	Participates in photoreceptor morphogenesis in the retina
CRYAA	Enhances the lens's transparency and refractive index.
CX3CR1	promotes cell survival by directing the recruitment of macrophages and monocytes to inflamed atherosclerotic plaques, acting as a regulator of the inflammatory process that leads to atherogenesis.
HAMP	hormone produced by the liver that serves as the primary circulation regulator of the distribution and absorption of iron throughout tissues.
PAX6	vital role in the development of the nose, eyes, central nervous system, and pancreas acting as a transcription factor.
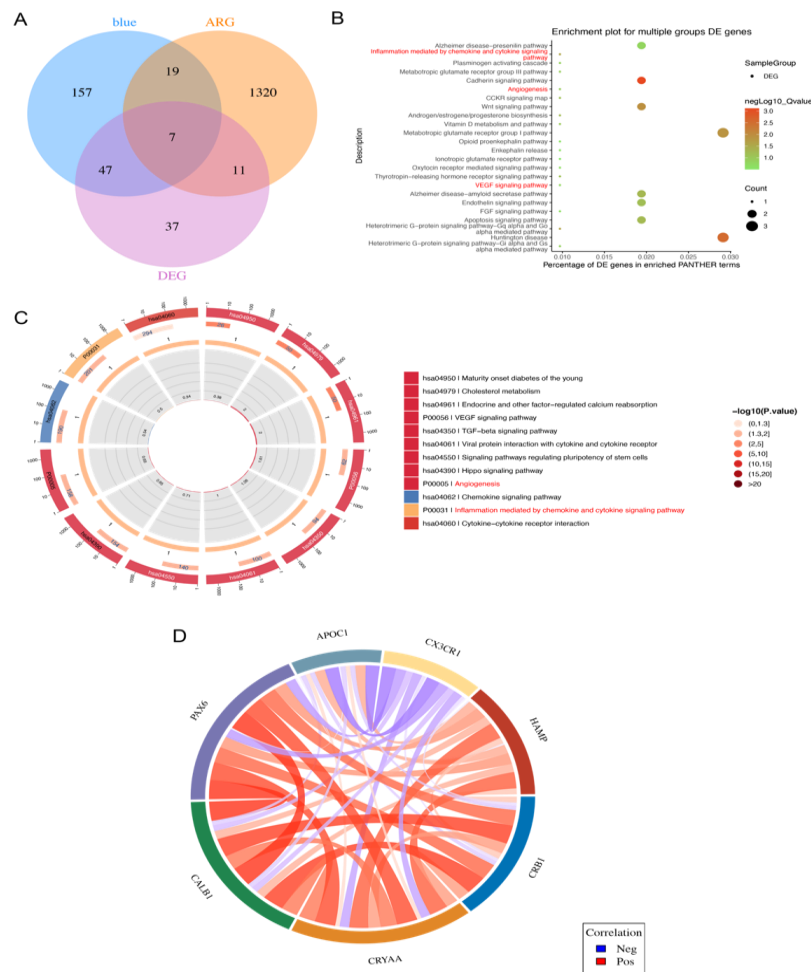
Figure 4: Identification and Functional Annotation of DEARGs in AMD. (A) A Venn diagram illustrating the intersection of DEGs, ARGs, and genes from the blue module. (B) KEGG disease enrichment analysis results for the DEARGs. (C) PANTHER enrichment analysis results for the DEARGs. (D) A STRING diagram depicting the interactions and correlations among the DEARGs.

3.4. Single-Cell Analysis and Subcellular Localization of Hub DEARGs

By using the single-cell analysis technique, we were able to precisely define the hub DEARGs' expression level in the human retina and locate the cell population that expresses these genes. The GEO dataset GSE155288's 6 samples that were equal distribution in the macular and peripheral retina were used for single cell analysis. Retinal and choroidal cell types' known gene markers were used to annotate cell clusters, and clusters that shared these markers were joined to create ten distinct cell types in total. These include photoreceptor cells (rod and cone cells); glial cells (Müller cell, astrocyte, microglia); neural cells (bipolar and ganglion cells), and vascular cells (pericyte and endothelial cells). We then plan to investigate the precise location of each of the hub genes. The findings indicate that microglia cells have the highest level of APOC1 expression (Figure 5A), CALB1 is in ganglion and cone cells (Figure 5B), CRB1 is in cone cells (Figure 5C), HAMP is in microglia cells (Figure 5D), and PAX6 in Muller and ganglion cells (Figure 5E), while the location of the other 2 genes remains inconclusive due to shortness of samples available. Further subcellular analysis of these 7 hub genes was carried out to find the precise location of each of the genes. The following bar chart of each gene shows the results. For the Gene APOC1 (Figure 5F) and CRB1 (Figure 5H), they are shown to be

most abundant in the extracellular region; for CALB1 it is the nucleus (Figure 5G); for PAX6 (Figure 5J), it is located in the cytoplasm and nucleus; for HAMP (Figure 5I), it is in the plasma membrane.
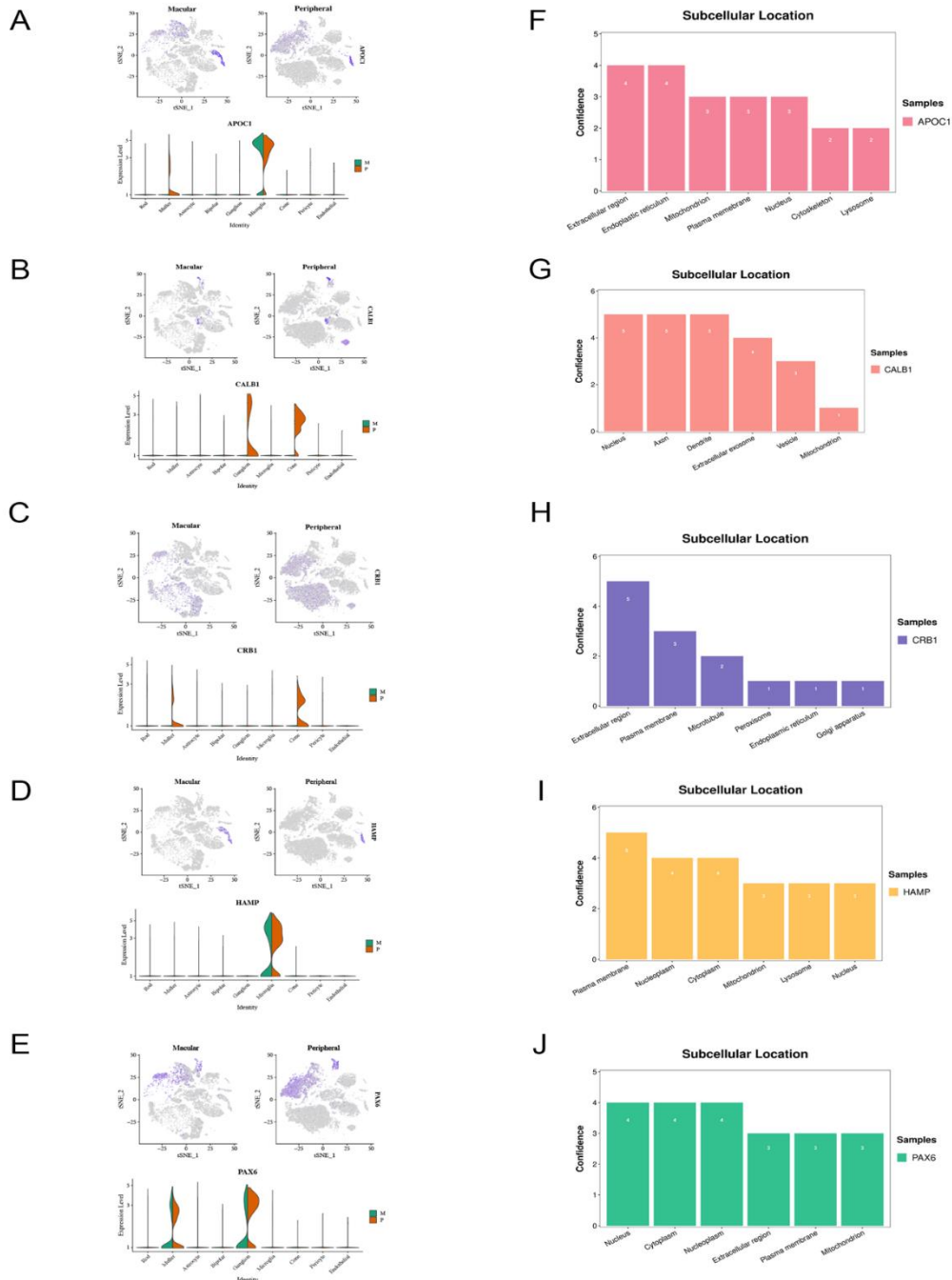
Figure 5: Single-Cell Analysis and Subcellular Localization of Hub DEARGs. (A-E) Single-cell expression analysis for the following genes: (A) APOC1, (B) CALB1, (C) CRB1, (D) HAMP, (E) PAX6. (F-J) Subcellular localization analysis for the genes: (F) APOC1, (G) CALB1, (H) CRB1, (I) HAMP, (J) PAX6.

3.5. Analysis of Immune Cell Infiltration

Considering that 2 of the 7 DEARGs we found were related to immune cells and the reason that the cause of the AMD is highly related to inflammation, A cell infiltration analysis was undertaken on

the samples. The immune cells were divided into 2 layers according to their specificity, where Top layer cells included DC, B cell, monocyte, macrophage, NK, neutrophil, CD4 T, CD8 T, NKT, Tgd, and bottom layer cells included Tc, Tex, Tr1, nTreg, iTreg, Th1, Th2, Th17, Tfh, Tcm, Tem, MAIT (Figure 6A). The immune cell percentages were displayed by each histogram's colors. The findings reveal that there was significant infiltration of DC, B cells, monocytes, macrophages, NK cells, neutrophils, CD4 T cells, CD8 T cells, NKT cells, and gamma delta cells and each was present in 57 out of a total of 58 samples. The correlation of immune cell infiltration between AMD clinical traits was also explored and the results are shown in the box plot below. By focusing on the plots that attained a p-value less than 0.05, it is found that the infiltration levels of macrophage, neutrophile, and MAIT cells were significantly altered, with macrophage increases and the other two decreases (Figure 6B). While this is so, all types of lymphocytic cells remain unchanged, revealing the fact that the inflammation occurring during AMD is due to the malfunction of the phagocytes regardless of the lymphocyte.
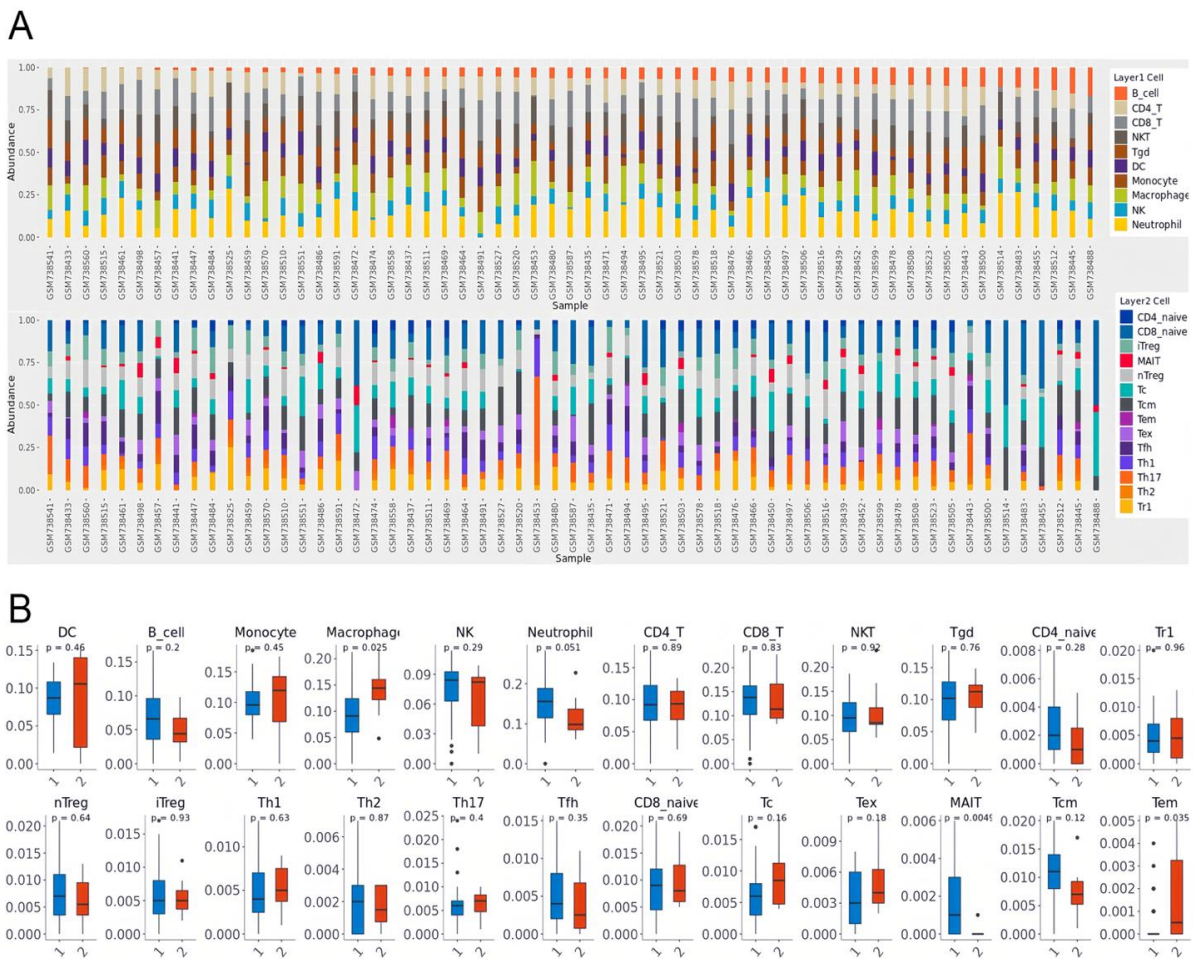
Figure 6: Analysis of Immune Cell Infiltration. (A) Percentage representation of each immune cell type from the two layers across samples. (B) Difference of immune cell types' expression levels in Group 1 (control group) and Group 2 (AMD patients).

3.6. Correlation Analysis Between Hub DEARGs and Immune Cells

After receiving the result of the differentially infiltrated immune cells, we plan to find the specific correlation of these immune cells with our DEARGs. We discovered that APOC1 and CX3CR1, two

hub genes linked to immunology, were substantially related to all immune cell types through immunological infiltration for individual genes. The most prominent result is the negative correlation between the two genes and macrophage cells M0, M1, and M2 (Figure 7A, B). These findings might prove their importance to the malfunction of the immune system during AMD inflammation pathogenesis. With the aforementioned data, we continue to explore these two immune-related hub genes. Through assessing their individual expression difference in various types of cancers, we found that the two genes were simultaneously up-regulated in most cancers. For APOC1, it is up regulated in 22 out of the total 33 enlisted cancers (Figure 7C); for CX3CR1, it is up regulated in 6 of the 7 cancers where it is differentially expressed (Figure 7D). This result may add to the explanation of the differential expression between these two immune-related genes in AMD.
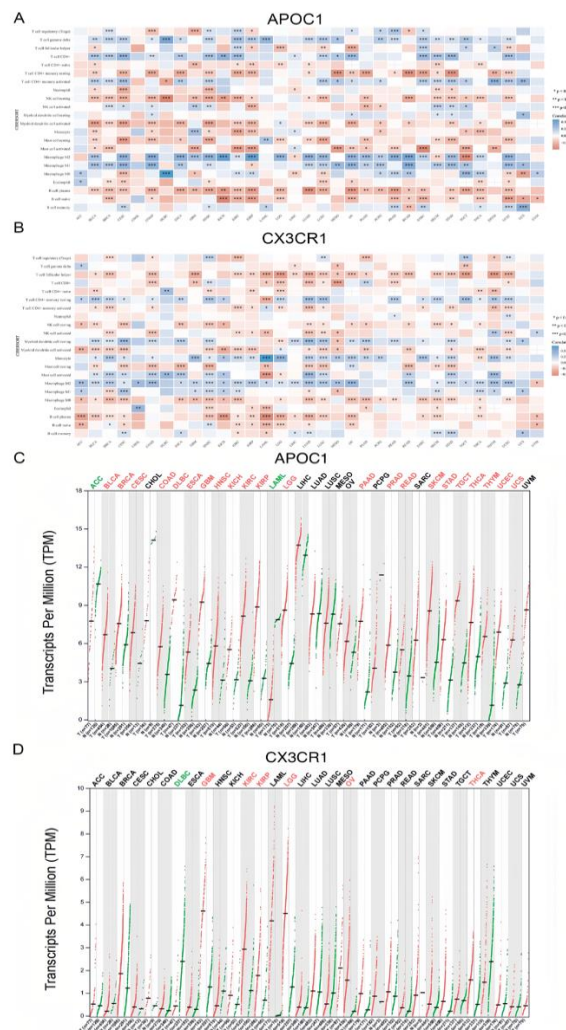
Figure 7: Correlation of Hub DEARGs with Immune Cells and Pan-Cancer Analysis. (A) Correlation analysis between the gene APOC1 and various immune cells. (B) Correlation analysis between the gene CX3CR1 and various immune cells. (C) Pan-cancer analysis results for the gene APOC1. (D) Pan-cancer analysis results for the gene CX3CR1.

3.7. Analysis of Protein Networks Among DEARGs and Their Functions

In order to study more about hub DEARGs linked to AMD and their related mechanisms, we used the STRING website by uploading the 7 identified genes and created a PPI network. The result shows

that they were 1 potential pathway among our group of DEARGs, which includes the genes CRYAA, PAX6, and CALB1 (Figure 8A). Henceforth, to further explore these three genes' protein connections, we examined the protein domains of these three interacting proteins. We give an estimation that the location of the interaction of the proteins would be within the protein domains, considering the fact that the protein domains were the main structure of the entire protein (Figure 8B). The results are shown in the graph below, and this information will be used in the further development of this study. With the identified protein network, we continued to explore this specific route's functions. Through functional enrichment analysis, it is shown that these connecting proteins were important for the functions of eye photoreceptor cell development, negative regulation of neurogenesis, retina layer formation, and eye development (Figure 8C). Their subcellular regions were also marked through enrichment which overlapped with our past results.
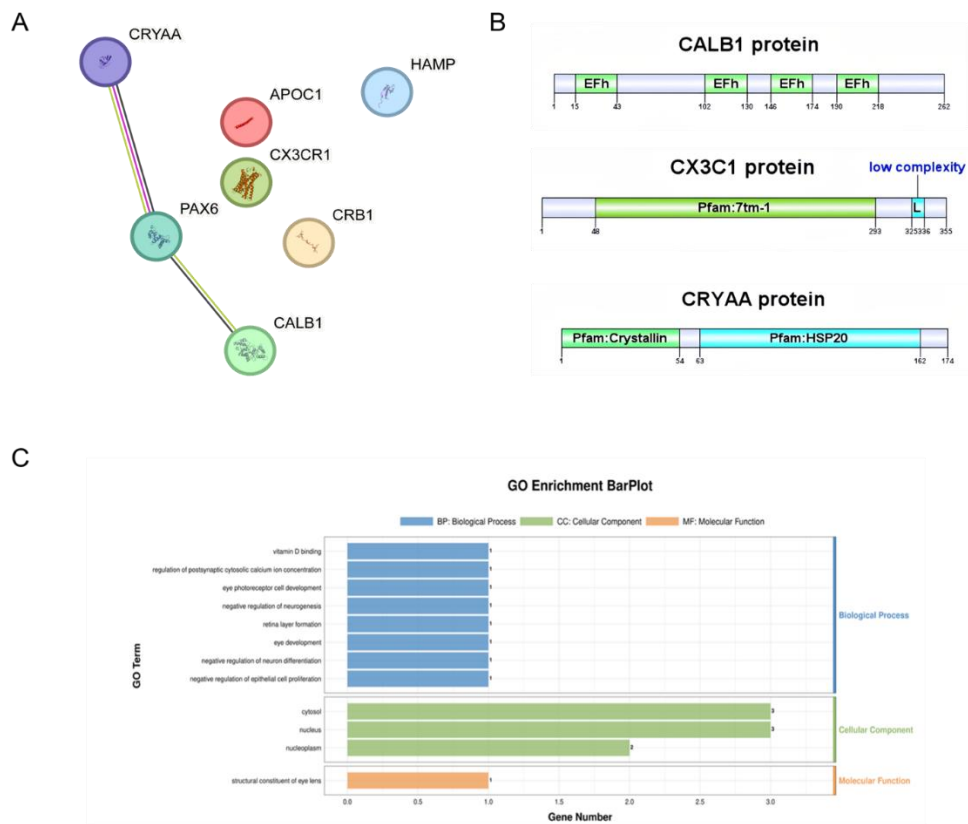
Figure 8: DEARGs Protein Networks and Interacting Protein Domains. (A) Protein-protein interaction network of DEARGs. (B) Specific protein domains of the interacting proteins, with domain positions indicated. (C) Functional enrichment analysis for the protein network using the Gene Ontology (GO) database.

3.8. Prediction of Protein-Protein Interactions

By using the AlphFold server, we predicted the interaction of the three proteins. Figure 9A shows the predicted structure of the protein from genes CRYAA and PAX6 where the red protein chain is from PAX6 and the blue one is from CRYAA. While Figure 9C shows the predicted structure from the genes PAX6 and CALB1 where the yellow chain is from CALB1 and the white one is oriented from PAX6. It is evident from the 3D models that there are several polar connections between the two molecules of each production, which confirms our estimation of their linkage. Furthermore, the position of the interacting location was compared, and was confirmed that they are within each

protein's domains, which could explain the pattern formed by the expected position error graph (Figure 9 B, D) owing to the functioning structure of the protein were its domain.
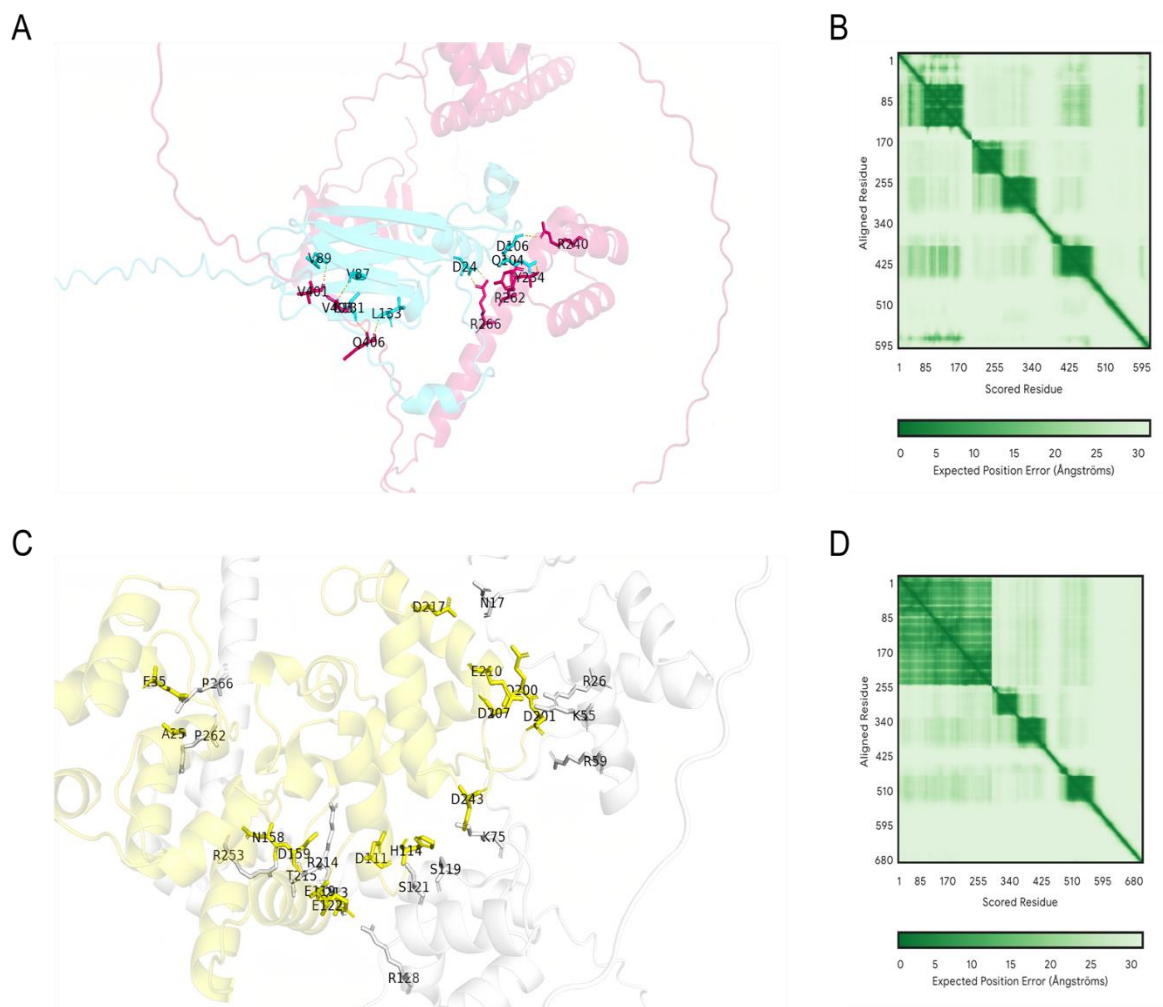
Figure 9: Prediction of Protein-Protein Interactions and Model Accuracy. (A) Predicted 3D structure of the interaction between PAX6 and CRYAA proteins, with CRYAA depicted in blue and PAX6 in red. (B) Corresponding error expectation for the PAX6-CRYAA model. (C) Predicted model of the interaction between PAX6 and CALB1 proteins, with PAX6 shown as the white chain and CALB1 as the yellow chain. (D) Corresponding error expectation for the PAX6-CALB1 model.

3.9. Drug-Protein Interaction Analysis via Molecular Docking and Target Drug Selection for DEARGs

Devising potential drugs that could specifically focus on targeting these identified hub genes offers a new strategy for treating AMD. With this agenda in mind, we set out to find small-molecule medicines recorded in the PubChem database that fit our description of targeting these genes. Three drugs were found, targeting the genes CRYAA, CX3CR1, and HAMP respectively. These drugs were chosen based on the chemicals and bioactivities sections in the PubChem database. Next, the binding potential was appraised by docking these three bioactive chemicals with the proteins from the gene CRYAA (Figure 10A), CX3CR1 (Figure 10B) and HAMP (Figure 10C). The figures below show the predicted 3D models of the docking of each protein and their respective drug. The models with the most accurate predictions were saved and edited by PyMol to further clarify the interaction between

the proteins and the molecules. The firm polar bonding of the first two proteins with the drug indicates and the hydrophobic interaction of the last protein supports the idea that they can slow down or possibly inhibit AMD from developing. Even though here we only shown three models of protein-drug docking analysis, we have still found other drugs that may be potentially used to target our DEARGs. However, due to the lack of sufficient molecular 3D structure, docking analysis were prohibited. Hence, a list was drawn to show all the relevant drugs we have found (Table 3).
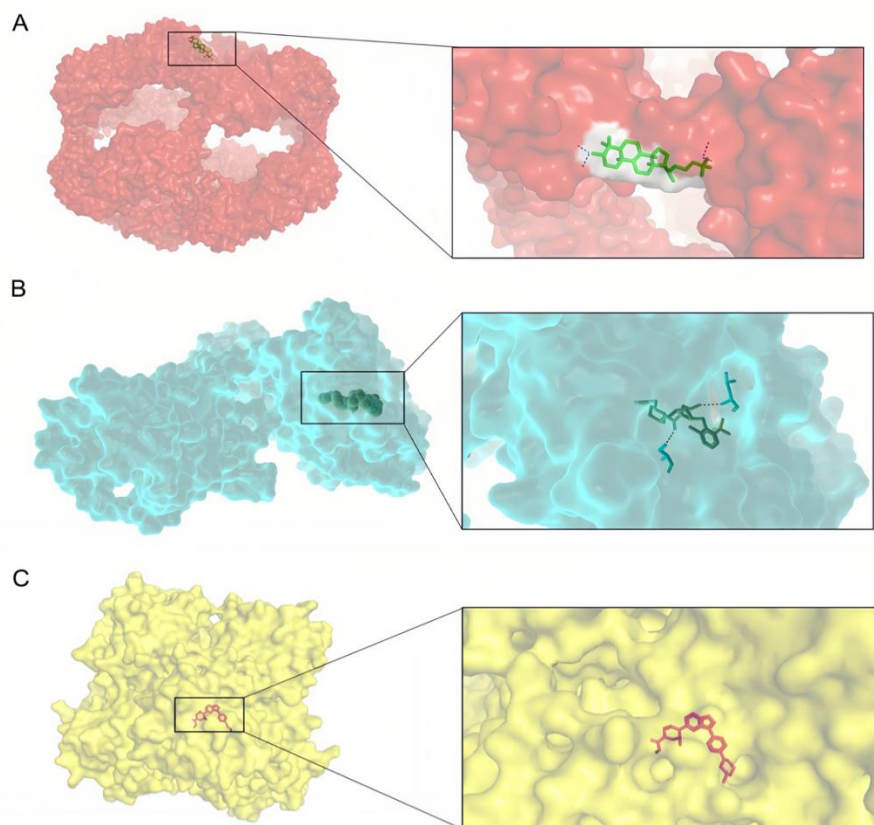
Figure 10: Drug-Protein Interaction Analysis and Target Drug Selection for DEARGs via Molecular Docking. Molecular docking models for the proteins: (A) CRYAA, (B) CX3CR1, and (C) HAMP.

Table 3: Information on Potential Drugs Targeting Biomarkers

Drug Names	Target	Origin
ALN-HPN	hepcidin antimicrobial peptide	Chemical, synthetic, nucleic acid
aniridia therapy	paired box 6	Biological, nucleic acid, viral vector
anti-CX3CR1 antibody	C-X3-C motif chemokine receptor 1	Biological, protein, antibody
CAP 1160	crystallin alpha A	Chemical, synthetic
Pax gene therapy	paired box 4	Biological, nucleic acid, non-viral vector
DS 28120313	hepcidin antimicrobial peptide	Chemical, synthetic
DS 79182026	hepcidin antimicrobial peptide	Chemical, synthetic
hepcidin mimetics	hepcidin antimicrobial peptide	Chemical, synthetic, peptide

Table 3: (continued).

lexaptepid pegol	hepcidin antimicrobial peptide	Chemical, synthetic, nucleic acid
anti-hepcidin MAb	hepcidin antimicrobial peptide	Biological, protein, antibody
Pax4 func agonists	paired box 4	Chemical, synthetic
PRS-080#022-DP	hepcidin antimicrobial peptide	Biological, protein, recombinant
PN 8518A	hepcidin antimicrobial peptide	Chemical, synthetic, peptide
SAR 445611	C-X3-C motif chemokine receptor 1	Biological, protein, antibody
anaemia of inflammation antisense therapy	hemojuvelin BMP co-receptor	Chemical, synthetic, nucleic acid

4. Discussion

This study employed multiple bioinformatics technologies to investigate Age-Related Macular Degeneration (AMD) with the goal of identifying potential biomarkers for the disease. We accomplished this by first using datasets from the GEO database (GSE29801) to find genes that are differentially expressed and linked to AMD. We contrasted the gene expression profiles of the macular tissues of a representative group of AMD/CNV patients with those of healthy people. Seven up-regulated genes and ninety-six down-regulated genes made up the 103 DEGs that our analysis found. We next carried out functional enrichment analysis to validate these important DEGs' applicability to AMD. The association between these DEGs and AMD was emphasized by the Gene Ontology (GO) enrichment analysis results, which identified several pathways linked to ocular development. Additionally, the KEGG analysis indicated that immune responses may also play a role in the regulation of these DEGs, alongside several pathways related to growth and development. The emphasis on developmental and growth aspects of the DEGs was unexpected. However, further enrichment results from the PANTHER database reinforced this observation, revealing significant enrichment in processes related to development and inflammation. These findings support the hypothesis that immunological factors contribute secondarily to the onset of AMD, with inflammation and growth development identified as the primary drivers of the disease. Consequently, these DEGs may be potentially playing a critical role in the pathogenesis of AMD.

Following our initial gene expression analysis, we used Weighted Gene Co-Expression Network Analysis (WGCNA) to identify modules containing co-expressing genes relevant to AMD. This analysis revealed ten modules associated with the disease. Notably, the blue module emerged as the most significant, identified by correlating functional enrichment analysis with gene importance. The enrichment results for this module mirrored those of the DEGs, showing a strong association with AMD and a significant involvement of growth-related processes in disease development. After extracting publicly known aging-related genes (ARGs), we identified an intersection of 7 genes from the ARGs, DEGs, and the blue gene module. These genes are APOC1, CALB1, CRB1, CRYAA, CX3CR1, HAMP, and PAX6. Interestingly, few of these confirmed hub genes have been previously reported as significant to AMD, although some have been implicated in retinal development and retinal-related pathogenesis. This suggests that our findings may contribute to a deeper understanding of the molecular underpinnings of AMD and potentially uncover new therapeutic targets.

CALB1 (Calbindin 1) is a Ca^{2+} −binding protein along the NFAT pathway. Through research results, it is suggested that the elevated expression level of the Ca^{2+} −binding protein calbindins could be seen as a common indicator of senescent cells[18], which in the case of AMD, may be caused by the aging patients. CRB1 (Crumbs Cell Polarity Complex Component 1) contributes to the

development of photoreceptors in the retina. Additionally, previous research has suggested that CRB1, which is well known to induce retinal deterioration such as retinitis pigmentosa (RP) and Leber congenital amaurosis (LCA) [19, 20], hence it is possibly a major determinant in the degradation of RPE in AMD. Further research demonstrates that CRB1 mutation is also directly linked to damage in the outer blood-retinal barrier which could cause irreversible vision loss[21]. CRYAA (Crystallin Alpha A) is found as an enhancer of the lens's transparency and refractive index[22], and recent research has found that CRYAA produces peak expression at different stages during the development of the human embryonic retina. [23]. This may mean it is a regulator of retinal growth. HAMP (Hepcidin Antimicrobial Peptide) encodes for the protein hepcidin which tightly controls the human serum iron level and is devoted to maintaining iron homeostasis, by its regulation of ferroportin[24]. Logically, the malfunction of this gene may be associated with iron accumulation which promotes the senescence-associated secretory phenotype (SASP) and the production of reactive oxygen species, leading to cell senescence[25]. Remarkably, HAMP also controls the primary mechanisms by which iron is released into plasma, such as macrophages recycling iron by phagocytosing old erythrocytes and other cells [26]. PAX6 (Paired Box 6) is regarded as the eye's main regulator[27] and many other types of ocular abnormalities were reported to be related to PAX6 [28]. These aforementioned genes were all related to the development of the eye as well as senescence processes that occurred during the pathogenesis of AMD.

This leaves 2 other hub genes, which were both highly related to immunology. APOC1 (Apolipoprotein C1) is used in the prognosis of various cancers as an abnormally expressed gene[29]. From pre-existing studies, we found that APOC1 also serves as an immunological biomarker for cancer and is mostly expressed in macrophages[30]. This piece of information is interesting as we further explored and found that elderly illnesses, such as AMD, are associated with pathogenic macrophage aging, which may cause damages such as declined autophagic ability[31] and declined phagocytic capacity[32]. Moreover, research evidence supports the pathogenic role of macrophages in AMD where activated macrophages generated from neovascular AMD patients exhibit proangiogenic features[33, 34]. The other immune-related gene is CX3CR1 (C-X3-C Motif Chemokine Receptor 1) is heavily expressed in blood monocytes, brain microglia cells, DC subsets, T-cell and natural killer (NK) cell subsets[35]. While increased microglial activation, inflammation, vascular injury, and neuronal death were the outcomes of CX3CR1 deficiency [36], its reaction with its corresponding ligand CX3CL1 provides a vital survival signal, the lack of which causes a rise in the death of monocytes[37].

Building on our previous findings, we further investigated the specific cell types in which these DEARGs are expressed. Using single-cell analysis, we identified the cell types where the proteins of these DEARGs are predominantly expressed and determined their respective subcellular locations. Our results indicate that these hub DEARGs are commonly located within the plasma membrane of ocular cells. With the insight into the immunological relationship of our hub genes, we proceeded to delve deeper into this aspect using immune cell infiltration analysis. We discovered that while the overall number of lymphocytic cells remained unchanged, AMD patients exhibited reduced levels of macrophage cells and MAIT cells. These findings suggest that the inflammation associated with AMD pathogenesis is not primarily driven by adaptive immunity mediated by lymphocytes but is instead attributed to the dysfunction of the innate immune system.

Following this idea, we continued to look deeper into the interrelation of the two hub genes related to immunity and the immune cells. Through using data from pan-cancer analysis, the data showed that the gene APOC1 and CX3CR1 are both highly correlated to multiple forms of cancerous immune cells, where their negative correlation with the macrophage is most conspicuous. This means that both genes suppress the expression of macrophage cells. The 2 immune-related genes were shown to function poorly in regions other than the eye, according to the Pan-Cancer Analysis, which also

reveals that these genes are typically dysregulated in a variety of malignancies, in contrast to their expression in AMD. In conjunction with the information, we gather from GEPIA, we derive a rationale that in malignancies, immune-related hub genes were up-regulated to inhibit macrophage expression and prevent them from clearing out cancerous cells, and in AMD, the two genes were down-regulated to promote the expression of macrophage and inducing inflammation responses. In the pathogenesis of AMD, macular fibrosis is present as the last phase[38], and intriguingly, we found past research showing that myofibroblasts are essential cells in the formation of fibrosis[39], and macrophages can differentiate into these myofibroblast-like cells[40]. This could fully add to our explanation of the immune-related hub gene theory, where aging dampens the expression level of these two immune-related hub genes and promotes the presence of the macrophage, ending in AMD inflammation pathogenesis and macular fibrosis.

Moreover, we looked into the potential pathway among our other DEARGs. Using PPI analysis, it is revealed that there exists a potential protein connection between the gene CRYAA, PAX6, and CALB1. To confirm this finding, we used AlphaFold prediction and displayed the polar interaction which confirm the stability and reality of the protein network. Moreover, we then employed further GO functional enrichment analysis on this network and found that it is related to eye development and eye photoreceptor cell development. Another enrichment result from the PANTHER database states clearly that this protein pathway is associated with angiogenesis and the VEGF signaling pathway, which could conclude this pathway is devoted to the formation of the AMD pathogenesis and hallmark, choroidal neovascularization. Finally, we identified three possible therapeutic drugs that target hub DEARGs, presenting an idea for AMD treatment. Subsequent molecular dockings provide precise molecule binding structures and enhance the validity of this suggestion. More potential therapeutic drugs were collected, however owing to the limit of information, further molecular docking reassurance was prohibited. Nevertheless, solely the presence of these target drugs for our identified biomarkers ensured their potential to be a target for future drugs. Hence, a list was drawn to reveal the public details of these potential drugs.

Despite our efforts, our research still contains several limitations. This research was limited to transcriptomics owing to the difficulty of attaining samples for experiments that rely heavily on post-mortem donations. This complex situation with the sample results in less abundance of the numbers of orienting samples and omics of our used data. Other latent direction of confirming the correctness of our analysis is experimenting through animal models, which is high-costs demanding, irreversible and the mechanism in the animal models may be inconsistent with that in humans. In addition, AMD is a heterogeneous disease in which the expression levels between patients are dissimilar, thus the DEG threshold value has been reduced in consideration of this aspect. In conclusion, this research used bioinformatic analysis to identify seven potential age-related biomarkers and two pathogenesis pathways of AMD where one leads to inflammation responses through the proliferation of macrophage, and the other leads to the formation of choroidal neovascularization through malfunction of growth regulator genes. By focusing on these possible biomarkers, future therapeutic strategies may be developed that aim to the aging cause of AMD.

References

[1] Fleckenstein, M., Keenan, T. D. L., Guymer, R. H., Chakravarthy, U., Schmitz-Valckenberg, S., Klaver, C. C., Wong, W. T. and Chew, E. Y. (2021) Age-related macular degeneration. Nature Reviews. Disease Primers, 7(1), 31.

[2] Cheung, G. C. M., Lai, T. Y. Y., Gomi, F., Ruamviboonsuk, P., Koh, A. and Lee, W. K. (2017) Anti-VEGF Therapy for Neovascular AMD and Polypoidal Choroidal Vasculopathy. Asia-Pacific Journal of Ophthalmolog, 6(6), 527–534.

[3] Hussain, R. M. and Ciulla, T. A. (2017) Emerging vascular endothelial growth factor antagonists to treat neovascular age-related macular degeneration. Expert Opinion on Emerging Drugs, 22(3), 235–246

[4] Barrett, T., Wilhite, S. E., Ledoux, P., Evangelista, C., Kim, I. F., Tomashevsky, M., Marshall, K. A., Phillippy, K. H., Sherman, P. M., Holko, M., Yefanov, A., Lee, H., Zhang, N., Robertson, C. L., Serova, N., Davis, S. and Soboleva, A. (2013) NCBI GEO: archive for functional genomics data sets--update. Nucleic Acids Research, 41, D991–D995.

[5] Langfelder, P. and Horvath, S. (2008). WGCNA: an R package for weighted correlation network analysis. BMC Bioinformatics, 9, 559.

[6] Zhang, B. and Horvath, S. (2005) A general framework for weighted gene co-expression network analysis. Statistical Applications in Genetics and Molecular Biology, 4, Article17.

[7] Thomas, P. D., Ebert, D., Muruganujan, A., Mushayahama, T., Albou, L. P. and Mi, H. (2022) PANTHER: Making genome-scale phylogenetics accessible to all. Protein Science : a Publication of the Protein Society, 31(1), 8–22.

[8] Kanehisa, M. and Goto, S. (2000) KEGG: kyoto encyclopedia of genes and genomes. Nucleic Acids Research, 28(1), 27–30.

[9] Liu, X., Jin, S., Hu, S., Li, R., Pan, H., Liu, Y., Lai, P., Xu, D., Sun, J., Liu, Z., Gao, Y., Zhao, Y., Liu, F., Xiao, Y., Li, Y., Wen, Y., Chen, Z., Xu, B., Lin, Y., Ran, M., Li, Q., Yang, S., Li, H., Tu, P., Haniffa, M., Teichmann, S., Bai, F. and Wang, Y. (2022) Single-cell transcriptomics links malignant T cells to the tumor immune landscape in cutaneous T cell lymphoma. Nature Communications, 13(1), 1158.

[10] Miao, Y. R., Zhang, Q., Lei, Q., Luo, M., Xie, G. Y., Wang, H. and Guo, A. Y. (2020) ImmuCellAI: A Unique Method for Comprehensive T-Cell Subsets Abundance Prediction and its Application in Cancer Immunotherapy. Advanced Science, 7(7), 1902880.

[11] Newman, A. M., Liu, C. L., Green, M. R., Gentles, A. J., Feng, W., Xu, Y., Hoang, C. D., Diehn, M. and Alizadeh, A. A. (2015) Robust enumeration of cell subsets from tissue expression profiles. Nature Methods, 12(5), 453–457.

[12] Tang, Z., Kang, B., Li, C., Chen, T. and Zhang, Z. (2019) GEPIA2: an enhanced web server for large-scale expression profiling and interactive analysis. Nucleic Acids Research, 47(W1), W556–W560.

[13] UniProt Consortium (2019) UniProt: a worldwide hub of protein knowledge. Nucleic Acids Research, 47(D1), D506–D515. 14.

[14] Yates, A. D., Achuthan, P., Akanni, W., Allen, J., Allen, J., Alvarez-Jarreta, J., Amode, M. R., Armean, I. M., Azov, A. G., Bennett, R., Bhai, J., Billis, K., Boddu, S., Marugán, J. C., Cummins, C., Davidson, C., Dodiya, K., Fatima, R., Gall, A., Giron, C. G., Gil, L., Grego, T., Haggerty, L., Haskell, E., Hourlier, T., Izuogu, O. G., Janacek, S. H., Juettemann, T., Kay, M., Lavidas, I., Le, T., Lemos, D., Gonzalez Martinez, J., Maurel, T., McDowall, M., McMahon, A., Mohanan, S., Moore, B., Nuhn, M., Oheh, D. N., Parker, A., Parton, A., Patricio, M., Sakthivel, M. P., Salam, A. I. A., Schmitt, B. M., Schuilenburg, H., Sheppard, D., Sycheva, M., Szuba, M., Taylor, K., Thormann, A., Threadgold, G., Vullo, A., Walts, B., Winterbottom, A., Zadissa, A., Chakiachvili, M., Flint, B., Frankish, A., Hunt, S. E., IIsley, G., Kostadima, M., Langridge, N., Loveland, J. E., Martin, F. J., Morales, J., Mudge, J. M., Muffato, M., Perry, E., Ruffier, M., Trevanion, S. J., Cunningham, F., Howe, K. L., Zerbino, D. R. and Flicek, P. (2020). Ensembl 2020. Nucleic acids research, 48(D1), D682–D688.

[15] Abramson, J., Adler, J., Dunger, J., Evans, R., Green, T., Pritzel, A., Ronneberger, O., Willmore, L., Ballard, A. J., Bambrick, J., Bodenstein, S. W., Evans, D. A., Hung, C. C., O'Neill, M., Reiman, D., Tunyasuvunakool, K., Wu, Z., Žemgulytė, A., Arvaniti, E., Beattie, C., Bertolli, O., Bridgland, A., Cherepanov, A., Congreve, M., Cowen-Rivers, A., Cowie, A., Figurnov, M., Fuchs, F., Gladman, H., Jain, R., Khan, Y., Low, C., Perlin, K., Potapenko, A., Savy, P., Singh, S., Stecula, A., Thillaisundaram, A., Tong, C., Yakneen, S., Zhong, E., Zielinski, M., Žídek, A., Bapst, V., Kohli, P., Jaderberg, M., Hassabis, D. and Jumper, J. M. (2024) Accurate structure prediction of biomolecular interactions with AlphaFold 3. Nature, 630(8016), 493–500.

[16] Kim, S., Chen, J., Cheng, T., Gindulyte, A., He, J., He, S., Li, Q., Shoemaker, B. A., Thiessen, P. A., Yu, B., Zaslavsky, L., Zhang, J. and Bolton, E. E. (2023) PubChem 2023 update. Nucleic Acids Research, 51(D1), D1373–D1380.

[17] Morris, G. M., Huey, R., and Olson, A. J. (2008). Using AutoDock for ligand-receptor docking. Current protocols in bioinformatics, Chapter 8.

[18] Raynard, C., Tessier, N., Huna, A., Warnier, M., Flaman, J. M., Van Coppenolle, F., Ducreux, S., Martin, N. and Bernard, D. (2022) Expression of the Calcium-Binding Protein CALB1 Is Induced and Controls Intracellular Ca2+ Levels in Senescent Cells. International Journal of Molecular Sciences, 23(16), 9376.

[19] Ehrenberg, M., Pierce, E. A., Cox, G. F. and Fulton, A. B. (2013) CRB1: one gene, many phenotypes. Seminars in Ophthalmology, 28(5-6), 397–405.

[20] den Hollander, A. I., Ghiani, M., de Kok, Y. J., Wijnholds, J., Ballabio, A., Cremers, F. P. and Broccoli, V. (2002) Isolation of Crb1, a mouse homologue of Drosophila crumbs, and analysis of its expression pattern in eye and brain. Mechanisms of Development, 110(1-2), 203–207.

[21] Peng, S., Li, J. J., Song, W., Li, Y., Zeng, L., Liang, Q., Wen, X., Shang, H., Liu, K., Peng, P., Xue, W., Zou, B., Yang, L., Liang, J., Zhang, Z., Guo, S., Chen, T., Li, W., Jin, M., Xing, X. B., Wan, P., Liu, C., Lin, H., Wei, H., Lee, R. W. J., Zhang, Feng. and Wei, L. (2024). CRB1-associated retinal degeneration is dependent on bacterial translocation from the gut. Cell, 187(6), 1387–1401.e13.

[22] Richter, L., Flodman, P., Barria von-Bischhoffshausen, F., Burch, D., Brown, S., Nguyen, L., Turner, J., Spence, M. A. and Bateman, J. B. (2008) Clinical variability of autosomal dominant cataract, microcornea and corneal opacity and novel mutation in the alpha A crystallin gene (CRYAA). American Journal of Medical Genetics. Part A, 146A(7), 833–842.

[23] Zhang, S., Liu, C., Wang, Q., Zhou, H., Wu, H., Zhuang, J., Cao, Y., Shi, H., Zhang, J. and Wang, J. (2023) CRYAA and GJA8 promote visual development after whisker tactile deprivation. Heliyon, 9(3), e13897.

[24] Billesbølle, C. B., Azumaya, C. M., Kretsch, R. C., Powers, A. S., Gonen, S., Schneider, S., Arvedson, T., Dror, R. O., Cheng, Y. and Manglik, A. (2020) Structure of hepcidin-bound ferroportin reveals iron homeostatic mechanisms. Nature, 586(7831), 807–811.

[25] Maus, M., López-Polo, V., Mateo, L., Lafarga, M., Aguilera, M., De Lama, E., Meyer, K., Sola, A., Lopez-Martinez, C., López-Alonso, I., Guasch-Piqueras, M., Hernandez-Gonzalez, F., Chaib, S., Rovira, M., Sanchez, M., Faner, R., Agusti, A., Diéguez-Hurtado, R., Ortega, S., Manonelles, A., Engelhardt, S., Monteiro, F., Attolini, C., Prats, N., Albaiceta, G., Cruzado, J. and Serrano, M. (2023) Iron accumulation drives fibrosis, senescence and the senescence-associated secretory phenotype. Nature Metabolism, 5(12), 2111–2130.

[26] Ganz, T. and Nemeth, E. (2012) Hepcidin and iron homeostasis. Biochimica et Biophysica Acta, 1823(9), 1434–1443.

[27] Halder, G., Callaerts, P. and Gehring, W. J. (1995) Induction of ectopic eyes by targeted expression of the eyeless gene in Drosophila. Science, 267(5205), 1788–1792.

[28] Lima Cunha, D., Arno, G., Corton, M. and Moosajee, M. (2019) The Spectrum of PAX6 Mutations and Genotype-Phenotype Correlations in the Eye. Genes, 10(12), 1050.

[29] Zhang, H., Wang, Y., Liu, C., Li, W., Zhou, F., Wang, X. and Zheng, J. (2022) The Apolipoprotein C1 is involved in breast cancer progression via EMT and MAPK/JNK pathway. Pathology, Research and Practice, 229, 153746.

[30] Ren, L., Yi, J., Yang, Y., Li, W., Zheng, X., Liu, J., Li, S., Yang, H., Zhang, Y., Ge, B., Zhang, S., Fu, W., Dong, D., Du, G., Wang, X. and Wang, J. (2022) Systematic pan-cancer analysis identifies APOC1 as an immunological biomarker which regulates macrophage polarization and promotes tumor metastasis. Pharmacological Research, 183, 106376.

[31] Khalil, H., Tazi, M., Caution, K., Ahmed, A., Kanneganti, A., Assani, K., Kopp, B., Marsh, C., Dakhlallah, D. and Amer, A. O. (2016) Aging is associated with hypermethylation of autophagy genes in macrophages. Epigenetics, 11(5), 381–388.

[32] Wong, C. K., Smith, C. A., Sakamoto, K., Kaminski, N., Koff, J. L. and Goldstein, D. R. (2017). Aging Impairs Alveolar Macrophage Phagocytosis and Increases Influenza-Induced Mortality in Mice. Journal of immunology, 199(3), 1060–1068.

[33] Hagbi-Levi, S., Grunin, M., Jaouni, T., Tiosano, L., Rinsky, B., Elbaz-Hayoun, S., Peled, A. and Chowers, I. (2017) Proangiogenic characteristics of activated macrophages from patients with age-related macular degeneration. Neurobiology of Aging, 51, 71–82.

[34] Nakamura, R., Sene, A., Santeford, A., Gdoura, A., Kubota, S., Zapata, N. and Apte, R. S. (2015) IL10-driven STAT3 signalling in senescent macrophages promotes pathological eye angiogenesis. Nature Communications, 6, 7847.

[35] Imai, T., Hieshima, K., Haskell, C., Baba, M., Nagira, M., Nishimura, M., Kakizaki, M., Takagi, S., Nomiyama, H., Schall, T. J. and Yoshie, O. (1997) Identification and molecular characterization of fractalkine receptor CX3CR1, which mediates both leukocyte migration and adhesion. Cell, 91(4), 521–530.

[36] Beli, E., Dominguez, J. M., 2nd, Hu, P., Thinschmidt, J. S., Caballero, S., Li Calzi, S., Luo, D., Shanmugam, S., Salazar, T. E., Duan, Y., Boulton, M. E., Mohr, S., Abcouwer, S. F., Saban, D. R., Harrison, J. K. and Grant, M. B. (2016) CX3CR1 deficiency accelerates the development of retinopathy in a rodent model of type 1 diabetes. Journal of Molecular Medicine, 94(11), 1255–1265.

[37] Landsman, L., Bar-On, L., Zernecke, A., Kim, K. W., Krauthgamer, R., Shagdarsuren, E., Lira, S. A., Weissman, I. L., Weber, C. and Jung, S. (2009) CX3CR1 is required for monocyte homeostasis and atherogenesis by promoting cell survival. Blood, 113(4), 963–972.

[38] Stevens, T. S., Bressler, N. M., Maguire, M. G., Bressler, S. B., Fine, S. L., Alexander, J., Phillips, D. A., Margherio, R. R., Murphy, P. L. and Schachat, A. P. (1997) Occult choroidal neovascularization in age-related macular degeneration. A natural history study. Archives of Ophthalmology, 115(3), 345–350.

[39] Little, K., Ma, J. H., Yang, N., Chen, M. and Xu, H. (2018) Myofibroblasts in macular fibrosis secondary to neovascular age-related macular degeneration - the potential sources and molecular cues for their recruitment and activation. EBioMedicine, 38, 283–291.

[40] Little, K., Llorián-Salvador, M., Tang, M., Du, X., Marry, S., Chen, M. and Xu, H. (2020) Macrophage to myofibroblast transition contributes to subretinal fibrosis secondary to neovascular age-related macular degeneration. Journal of Neuroinflammation, 17(1), 355.